bases (aryl oxide or butylamine) abstract protons, it occurs after the rate-determining step.

c. Synchronous Proton Transfer and Aryl Oxide Expulsion. Coupling proton transfer with aryl oxide expulsion avoids formation of the N-protonated amide. Such a transition structure should have a similar or slightly smaller ammonium ion fragment than a hydrogen-bonded complex. This mechanism should correlate catalysis with basicity more than with the hydrogen-bonding ability of a catalyst. In light of Su and Watson's data,[14] we discount this mechanism.

d. Proton Shuttle to Aryl Oxide. One can imagine a concerted pathway where the proton is transferred to the departing aryl oxide. Such a mechanism agrees with the Hammett study[3] and the hydrogen-bonding study,[14] but this mechanism requires the coupling of many motions.

3. Conclusion. We favor mechanism b with aryl oxide as the proton acceptor. Ether or butylamine may do the actual abstraction, provided that this activity occurs in a fast step after the rate-determining step. Does the proton transfer to aryl oxide occur in a separate step? We cannot imagine how aryl oxide accepts the proton without disrupting the strong hydrogen bonding between polyether and N-protonated amide. The tight ion pair must be an intermediate, with proton loss easier than reformation of a TI. The aryl oxide nucleofuge may either take a proton from an intermediary base to form the final phenol product, or it may abstract a proton directly from the N-protonated amide polyether complex (or a less complexed form).

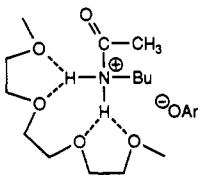

Summary

Glyme-catalyzed ester aminolysis in chlorobenzene shows transition-structure recognition in which a catalyst binds an ionic group that is attached to the site of reaction. *The number of ammonium protons in the transition structure determines both the number of polyether oxygens needed for optimal catalysis and the optimal spacing among these oxygens.* We have "fingerprinted" this ammonium ion by systematically varying the structure of ionophore catalysts and the number of protons in the ammonium ion of the transition structure. We offer the methods described above as paradigm for determining transition structure in aminolysis reactions.

Acknowledgment. We thank Mr. Don Patterson for technical assistance. We dearly thank Mrs. Mary Jane Peters for her encouragement.

Registry No. DME(3), 17081-21-9; DME(4), 13179-96-9; DME(5), 111-89-7; DME(6), 13179-98-1; DME(7), 137333-33-6; DME(8), 51306-09-3; DME(9), 91337-21-2; DME(10), 53759-62-9; DME(12), 73120-52-2; GLM(2), 110-71-4; GLM(3), 111-96-6; GLM(4), 112-49-2; GLM(5), 143-24-8; GLM(6), 1191-87-3; GLM(7), 1072-40-8; GLM(8), 1191-91-9; GLM(9), 25990-94-7; 1,3-propanediol, 504-63-2; 1,4-butanediol, 110-63-4; 1,5-pentanediol, 111-29-5; 1,6-hexanediol, 629-11-8; 1,7-heptanediol, 629-30-1; 1,8-octanediol, 629-41-4; 1,9-nonanediol, 3937-56-2; 1,10-decanediol, 112-47-0; 1,12-dodecanediol, 5675-51-4; 1,6-hexanediol ditosylate, 4672-50-8; 1,7-heptanediol ditosylate, 40235-95-8; 1,8-octanediol ditosylate, 36247-32-2; 1,9-nonanediol ditosylate, 73992-42-4; 1,10-decanediol ditosylate, 36247-33-3; 1,12-dodecanediol ditosylate, 36247-34-4; 4-nitrophenyl acetate, 830-03-5; butylamine, 109-73-9; methylbutylamine, 110-68-9.

Supplementary Material Available: Observed rate constants for polyether- and diether-catalyzed aminolysis of 4-nitrophenyl acetate at 25 °C in chlorobenzene (22 pages). Ordering information is given on any current masthead page.

Synthesis of Trioxatricornan and Derivatives. Useful Keystones for the Construction of Rigid Molecular Cavities

Michael Lofthagen, Russell VernonClark, Kim K. Baldridge,† and Jay S. Siegel*

Department of Chemistry, University of California, San Diego, La Jolla, California 92093, and San Diego Supercomputer Center, 10100 John Hopkins Ave., La Jolla, California 92137

Received August 13, 1991

The synthesis of a new class of organic keystones for the development of macrocage structures is presented. These represent some of the most versatile building blocks for macrocage construction. The keystone structure developed herein can be interpreted as either a centrally alkylated [*cd,mn*]dibenzopyrene or a tris ortho-bridged triphenylmethane. We call this basic skeleton tricornan. Routes into both chiral (C_3 and C_1 symmetry) and achiral (C_{3v} symmetry) derivatives are reported. The synthesis of derivatives of the trioxatricornan keystone, leading to two macrocage structures, is presented. The X-ray structures of *cent*-methyltrioxatricornan **7** and 2,6,10-tris(dimethylamino)-*cent*-methyltrioxatricornan (**20**) are discussed and compared to that of 1,1,1-triphenylethane. Empirical force field and AM1 calculations are compared to the X-ray structures and discussed. A general discussion on the keystone analogy is presented.

The idea of a molecular keystone, developed by Whitlock[1] and applied elegantly by Diederich[2] and Dougherty[3] to the molecular construction of binding sites for organic guest molecules, stems from the architectural design of a portal or archway.[4] The molecular keystone serves a versatile role; existing both as a structural basis for mo-

† San Diego Supercomputer Center.

(1) (a) Sheridan, R. E.; Whitlock, H. W., Jr. *J. Am. Chem. Soc.* **1986**, *108*, 7120. (b) Miller, S. P.; Whitlock, H. W., Jr. *J. Am. Chem. Soc.* **1984**, *106*, 1492. (c) Jarvi, E. T.; Whitlock, H. W., Jr. *J. Am. Chem. Soc.* **1982**, *104*, 7196.

0022-3263/92/1957-0061$03.00/0

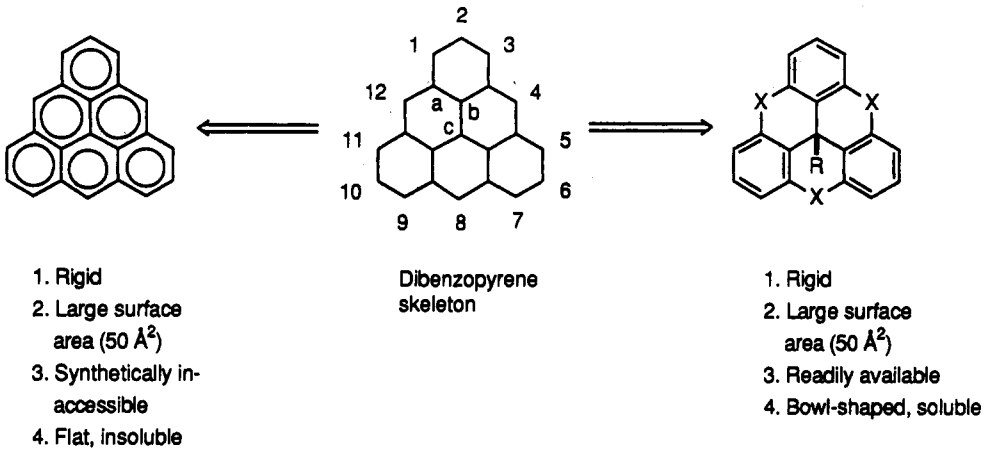

Figure 1. Design of a molecular structure based on the keystone principle.

Scheme I

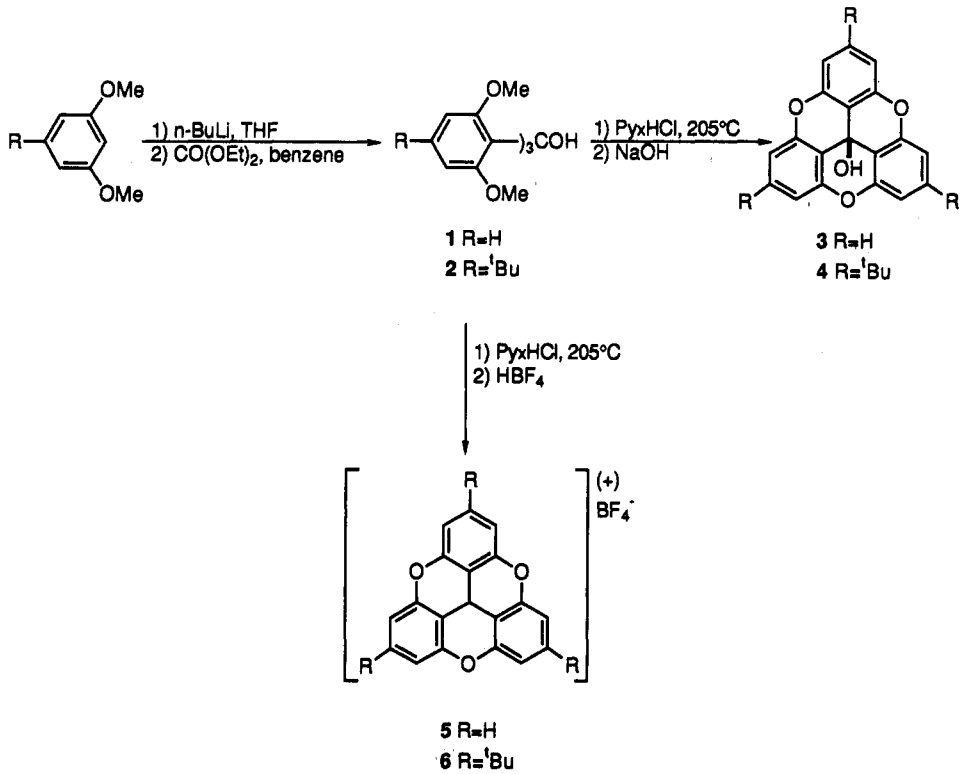

lecular cavities and as a site for the attachment of catalytic functionality. However, no system can be of general utility until a facile, large-scale synthesis leading into a number of derivatives is available.[5] We present such a staightforward synthetic scheme for a novel class of functionalized polycyclic aromatic structures, useful as molecular keystones.

Experimental Design

When designing a molecular structure based on the keystone principle, one strives for certain molecular properties (Figure 1): (1) preorganization;[6] (2) a large surface area;[7] (3) variable substitution patterns;[8] and (4) solubility.[9]

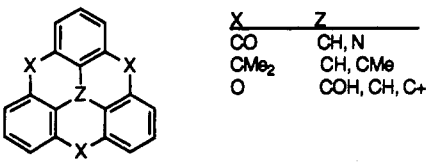

Figure 2. Derivatives of triangulene.

Figure 3. The parent keystones tricornan, and trioxatricornan.

(2) (a) Diederich, F.; Dick, K. *Angew. Chem., Int. Ed. Engl.* **1983**, *22*, 715. (b) Diederich, F.; Dick, K. *J. Am. Chem. Soc.* **1984**, *106*, 8024. (c) Diederich, F.; Griebel, D. *J. Am. Chem. Soc.* **1984**, *106*, 8037.

(3) (a) Petti, M. A.; Shepodd, T. J.; Dougherty, D. A. *Tetrahedron Lett.* **1986**, *27*, 807. (b) Shepodd, T. J.; Petti, M. A.; Dougherty, D. A. *J. Am. Chem. Soc.* **1986**, *108*, 6085.

(4) Webster's Ninth New Collegiate Dictionary; Mish, F. C., Ed.; Merriam-Webster: Springfield, 1986.

(5) Rebek, J.; Askew, B.; Killoran, M.; Nemeth, D.; Lin, F. T. *J. Am. Chem. Soc.* **1987**, *109*, 2426.

Scheme II

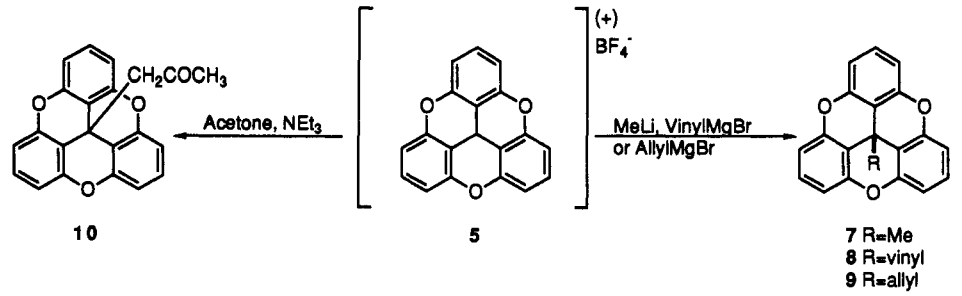

10 5 7 R=Me 8 R=vinyl 9 R=allyl

Scheme III

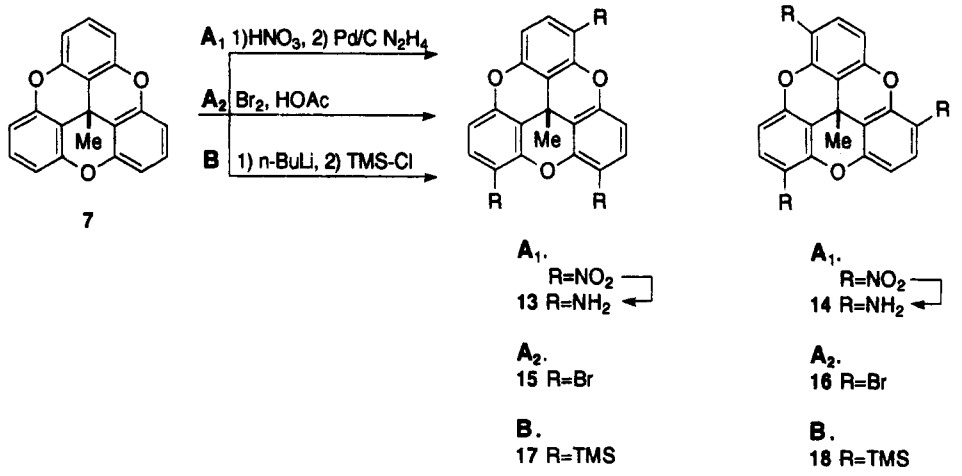

7

A1. R=NO2 → 13 R=NH2 ← A1. R=NO2 → 14 R=NH2 ←

A2. 15 R=Br A2. 16 R=Br

B. 17 R=TMS B. 18 R=TMS

The dibenzopyrene skeleton, for which Clar[10] coined the term triangulene, suffices as a starting template. Derivatives of triangulene with one or more sp^2-atoms replaced by sp^3-carbons or heteroatoms[11] have appeared in the literature (Figure 2). For example, one obtains the 4,8,12-trioxadibenzo[*cd*,*mn*]pyrene cation **5** in two steps starting from 1,3-dimethoxybenzene (Scheme I).[12] We have targeted additions to the central atom and substitution on the periphery of **5** as routes for development of keystones. Addition of H to the central carbon results in the compound we call trioxatricornan and its parent hydrocarbon is called tricornan (Figure 3).

The tricornan skeleton has three variable regions, x, y, and z (Figure 4). Region x is defined by positions 4, 8, and 12. Here, the electronic demands of the keystone can be regulated. Region y encompasses the radial and flanking positions on the aromatic rings. In this region bridging arms and/or functionality attach to the keystone. Substitution in region y modifies the symmetry; radial substitution on each ring results in C_{3v} symmetry, whereas

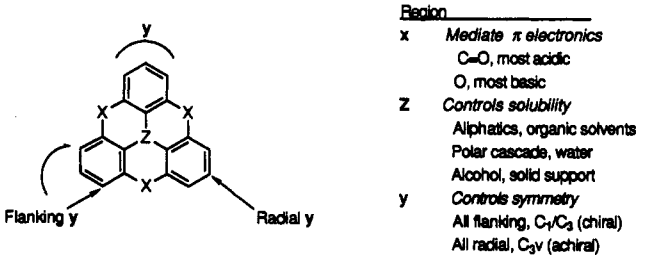

Figure 4. Regions x, y, and z of the triangulene nucleus.

substitution of one flanking position from each ring results in C_3 or C_1 symmetry. Region z stems directly from the central atom and involves the convex side of the keystone. This region can be extended to change the solubility of the keystone or to attach it to a solid support.[9]

Synthetic Approach

Previously, there have been modifications to both the x and z regions though little is known about modifications to region y. Restricting our discussion to the trioxatricornan family we present our routes to the modification of regions y and z.

Modification of region z is based on nucleophilic reactions at carbon 12c of Martin's salt (Scheme II). Precedence for this chemistry comes from studies on trityl cation.[13] Trityl cation alkylates weakly acidic compounds such as acetone and acetonitrile in the presence of a hindered base, and trityl alcohol reacts with trimethylaluminum to form triphenylethane.[14] Indeed, stabilized carbocations generally react with organometallic reagents.[15]

(6) (a) Breslow, R. *Isr. J. Chem.* **1979**, *18*, 187. (b) Cram, D. J. *Angew. Chem., Int. Ed. Engl.* **1986**, *25*, 1039.

(7) (a) Ferguson, S. B.; Seward, E. M.; Diederich, F.; Sanford, E. M.; Chou, A.; Inocencio-Szweda, P.; Knobler, C. B. *J. Org. Chem.* **1988**, *53*, 5593. (b) Haeg, M. E.; Whitlock, B. J.; Whitlock, H. W., Jr. *J. Am. Chem. Soc.* **1989**, *111*, 692.

(8) (a) Rebek, J., Jr. *Top. Curr. Chem.* **1988**, *149*, 189. (b) Diederich, F. *Angew. Chem., Int. Ed. Engl.* **1988**, *27*, 362.

(9) (a) Tomalia, D. A.; Baker, H.; Dewald, J.; Hall, M.; Kallos, G.; Martin S.; Roeck, J.; Ryder, J.; Smith, P. *Polym. J.* **1985**, *17*, 117. (b) Tomalia, D. A.; Naylor, A. M.; Goddard, W. A. *Angew. Chem., Int. Ed. Engl.* **1990**, *29*, 138. (c) Pirkle, W. H.; House, D. W. *J. Org. Chem.* **1979**, *44*, 1957.

(10) Clar, E.; Stewart, D. G. *J. Am. Chem. Soc.* **1953**, *75*, 2667.

(11) (a) Weiss, R.; Korczyn, J. *Monatsh* **1925**, *45*, 207. (b) Hellwinkel, D.; Aulmich, G.; Melan, M. *Chem. Ber.* **1981**, *114*, 86. (c) Hellwinkel, D.; Melan, M. *Chem. Ber.* **1974**, *107*, 616. (d) Hellwinkel, D.; Melan, M. *Chem. Ber.* **1971**, *104*, 1001. (e) Figuly, G. D.; Loop, C. K.; Martin, J. C. *J. Am. Chem. Soc.* **1989**, 111, 654.

(12) Martin, J. C.; Smith, R. G. *J. Am. Chem. Soc.* **1964**, *86*, 2252.

(13) Bidan, G.; Cauquis, G.; Genies, M. *Tetrahedron* **1979**, *35*, 177.

(14) Harney, D. W.; Meisters, A.; Mole, T. *Aust. J. Chem.* **1974**, *27*, 1639.

(15) (a) Top, S.; Jaouen, G. *J. Org. Chem.* **1981**, *46*, 78. (b) Semmelhack, M. F. *Ann. N. Y. Acad. Sci.* **1977**, *295*, 36. (c) Nicholas, K. M.; Mulvaney, M.; Bayer, M. *J. Am. Chem. Soc.* **1980**, *102*, 2508.

We have alkylated acetone with Martin's salt **5** using triethylamine as a base. We have also found that reagents such as methyllithium and vinyl and allyl grignard react with compound **5** in dry THF to place a methyl **7**, vinyl **8**, or allyl **9** group, respectively, in the 12c position (Scheme II).

The reaction with methyllithium is particularly facile and provides a model keystone **7** on which to perform further modifications of region Y. This derivative is quite soluble in a variety of organic solvents.

The vinyl group of **8** can be modified further. Hydroboration–oxidation of **8** with borane produces the primary and secondary alcohols in a ratio of 3.6:1.

With the keystone intact, many different pathways for incorporation of "handles" onto the corners of the trioxatricornan are possible.[16] We investigated two routes: electrophilic aromatic substitution and ortholithiation.

Electrophilic Substitution. Incorporation of three dissymetrically disposed "amino-handles" was achieved by electrophilic nitration of **7** followed by catalytic hydrogenation of the trinitrated keystones (Scheme III). The two regioisomeric triamines C_1 (**11**) and C_3 (**12**), that result from substitution at one flanking site on each benzene ring, were obtained in approximately a statistical ratio of 3:1 with a total yield of 36%. The two chiral regioisomers are easily separated on neutral alumina, with the more symmetric C_3 isomer eluting first.

Another route into chiral keystones involved electrophilic bromination of **7** (Scheme III). The tendency for 1,3-dimethoxybenzene to undergo overbromination[17] gave us reason to question this method. Nonetheless, bromination of **7** in neat glacial acetic acid produced the C_1/C_3 (**13, 14**) mixture with only a small amount of over brominated product. Crystallization from acetone yields the less soluble C_1 isomer **13**. The C_3 isomer, **14**, can be recovered easily from the C_3-enriched filtrate by column chromatography on silica.

Ortholithiation. In an attempt to achieve a different C_3/C_1 ratio, ortholithiation of **7** was investigated (Scheme III). Two facts led us to believe that the ortholithiation of trioxatricornans might be effected selectively with one substitution on each ring: (1) several heteroatom-directed ortholithiations have been reported in the literature,[18] oxygen being among the most common, and (2) dianions on single benzene rings are difficult to form.[19]

Treatment of **7** with excess *n*-BuLi in THF and quenching of the tri anion with TMSCl shows that only one deprotonation occurs per aromatic unit and that the directing power of the oxygens limits the number of regioisomeric products to the C_1, **15**, and C_3, **16**, isomers.[20] The C_1/C_3 ratio of 6:1 is higher than the expected statistical ratio of 6:2, indicating a preference for the pathway through the intramolecular dilithio aggregate.[23] A small amount of the C_s symmetric 3,5-bis(trimethylsilyl)-substituted *cent*-methyltrioxatricornan is seen.[24] The TMS mixture can be converted to the corresponding tribromides, **13** and **14**, by treatment with bromine in a THF solution.

Scheme IV

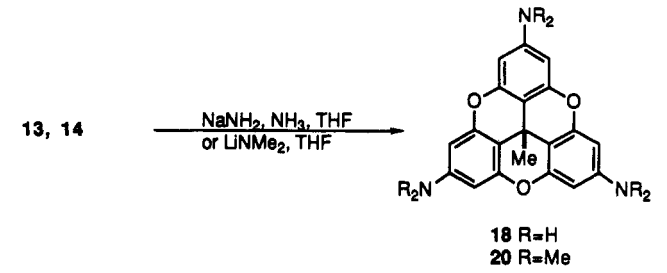

18 R=H
20 R=Me

Table I. ^{1}H NMR, ^{13}C{^{1}H} NMR and IR Data on Compounds 7, 11, 12, and 18

	^{1}H NMR[a]	^{13}C{H} NMR[b]	IR[c]
7	7.22, 6.92, 1.52	151.5, 128.8, 114.0, 111.4, 31.59 23.43	1608
18	6.23, 1.40	152.4, 149.0, 103.5, 96.51 32.27, 21.56	3456, 3371, 1627
12	6.75, 6.63, 1.52	142.3, 138.5, 132.4, 114.6 113.0, 110.0, 31.42, 24.80	3430, 3340, 1630
11	6.80–6.62, 1.54	142.8, 142.3, 141.8, 138.6 137.8, 137.7, 132.7, 132.4 131.9, 114.7, 114.6, 114.5 113.1, 112.8, 112.7, 110.5 110.2, 109.6, 31.49, 24.78	3380, 3310

[a] In $CDCl_3$ (ppm). [b] In DMSO-d_6 (ppm). [c] KBr pellets (cm^{-1}).

Cine Substitution. At first glance it might seem that these two pathways are restricted to mixtures of C_3 and C_1 isomers, leaving the all radial C_{3v} isomer unattainable. However, starting with the above described crude mixture of tribromides **13** and **14**, one effects a triple cine substitution[25] with sodium amide on the tri bromides and obtains the C_{3v} symmetric 2,6,10-triamino-*cent*-methyltrioxatricornan (**18**) as the sole regioisomer in 37% yield based on **7** (Scheme IV). Precedence for this procedure comes from the synthesis of 3,5-dimethoxyaniline.[17] The production of only this regioisomer, from a proposed benzyne intermediate, is a manifestation of the weaker basicity of the site ortho to the oxygen as is seen in the ortholithiation. Similarly, dimethylamide reacts via a cine substitution yielding the C_{3v} symmetric 2,6,10-tris(dimethylamino)-*cent*-methyltrioxatricornan (**20**).

The spectroscopic data for the three "triamines" C_{3v} (**18**), C_3 (**12**), and C_1 (**11**) and the parent keystone *cent*-methyltrioxatricornan (**7**) are presented in Table I.

Each of these isomers C_{3v}, C_3, and C_1 can serve in the design of molecular cavities.[26] Below we present two examples based on the C_{3v} symmetric triamine.

Formation of Cyclophanes. Tosylation of the triamine **18** gives an entry point into alkylation chemistry at nitrogen (Scheme V). Alkylation of **21** is affected by heating a mixture of the tosylated "triamine", alkylating agent, and

(16) The sole change in region Y that we could find in the literature was replacement of *tert*-butyl for H in positions 2, 6, and 10. This substitution pattern, reported by Peters, was affected by beginning with the *tert*-butyldimethoxybenzene. See: Peters, N. PhD dissertation, University of Illinois at Urbana Champaign, 1980, p 101.

(17) Benkeser, R. A.; Hickner, R. A.; Hoke, D. I.; Thomas, O. H. *J. Am. Chem. Soc.* **1958**, *80*, 5289.

(18) (a) Gschwend, H. W.; Rodriguez, H. R. *Org. React.* **1979**, *26*, 1. (b) Gilman, H.; Morton, J. W., Jr. *Org. React.* **1956**, *8*, 256. (c) Wakefield, B. J. *Organolithium Methods*; Academic Press: New York, 1988; p 189.

(19) Gilman, H.; Stuckwisch, C. G. *J. Am. Chem. Soc.* **1943**, *65*, 1461.

(20) In a similar fashion, dibenzofuran can be monolithiated in the 4-position[21a] or diphenyl ether can be dilithiated in the 2,2′-positions.[21b] Also, the lithiation reaction of dibenzo-1,4-dioxan has been reported to give the 1,9-dilithio product.[22]

(21) (a) Gilman, H.; Gorsich, R. D. *J. Org. Chem.* **1957**, *22*, 687. (b) Oita, K.; Gilman, H. *J. Am. Chem. Soc.* **1957**, *79*, 339.

(22) Palmer, B. D.; Boyd, M.; Denny, W. A. *J. Org. Chem.* **1990**, *55*, 438.

(23) Similar directing effects have been seen in the deprotonation of, e.g., 2-lithiobiphenyl, 1-lithionaphthalene, and 9-lithioanthracene: (a) Mitteil, I.; Neugebauer, W.; Schleyer, P. v. R. *J. Organomet. Chem.* **1982**, *228*, 107. (b) Neugebauer, W.; Clark, T.; Schleyer, P. v. R. *Chem. Ber.* **1983**, *116*, 3283.

(24) Regiochemistry determined by 1-D difference NOE experiments.

(25) (a) Hoffman, R. W. *Dehydrobenzene and Cycloalkynes*; Academic Press: New York, 1969. (b) Xin, H. Y.; Biehl, E. R. *J. Org. Chem.* **1983**, *48*, 4397.

(26) The C_3 isomer can form a D_3, C_3, or C_3h dimeric cage, which is an out-out, out-in, in-out, or in-in isomer. (a) Simmons, H. E.; Park, C. H. *J. Am. Chem. Soc.* **1968**, *90*, 2428. (b) Franke, J.; Vogtle, F. *Angew. Chem., Int. Ed. Engl.* **1985**, *24*, 219.

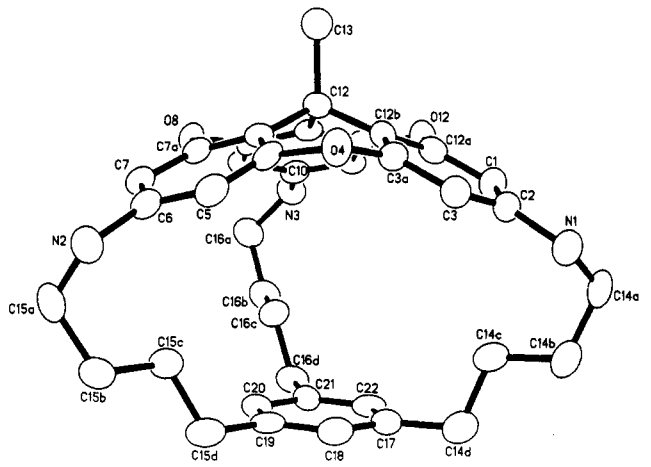

Figure 5. Structure of the macrocyclophane **23**.

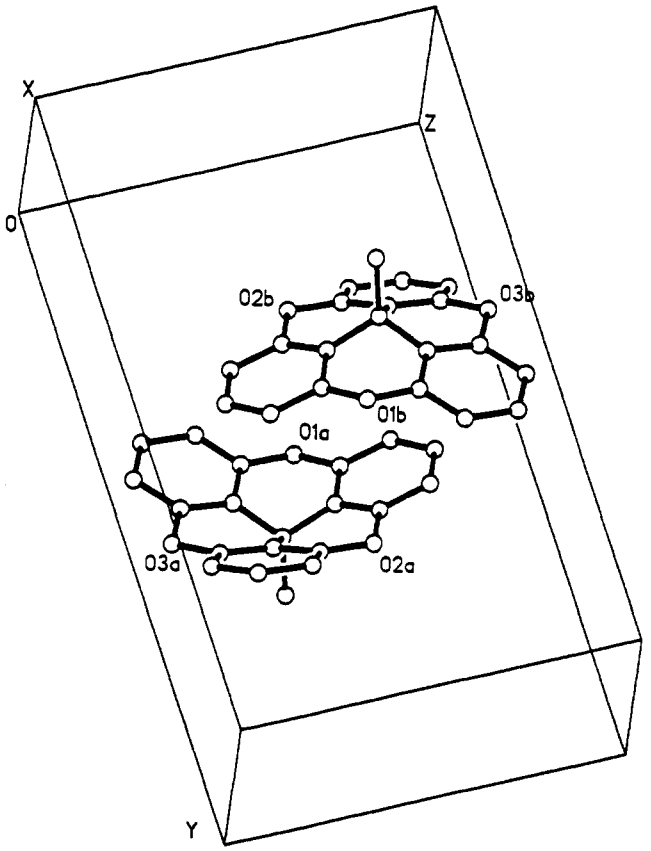

Figure 6. Unit cell diagram of **7**.

potassium carbonate at 70 °C in DMF for 16 h. A particularly useful alkylation is the reaction of **21** with a "Gabriel" protected α,Ω-aminohaloalkane to form an extended triamine after deprotection.

A novel type of cage structure can then be accessed by forming the amide with a benzyl-protected 2,3-dihydroxybenzoyl chloride followed by deprotection, i.e., hydrogenolysis, to give **22** (Scheme V). Treatment of **22** with iron(III) creates a siderophore/keystone macrocage hybrid.[27]

Another macrocage can be accessed by alkylation of **21** with 6-hexynyl-*p*-toluenesufonate followed by a [2 + 2 + 2] cyclization with Vollhardt's catalyst which yields the macrocage structures **23** and **24** (Scheme VI). **23** was shown by X-ray analysis and conformational analysis using

(27) Lofthagen, M.; Siegel, J. S. Manuscript in preparation.

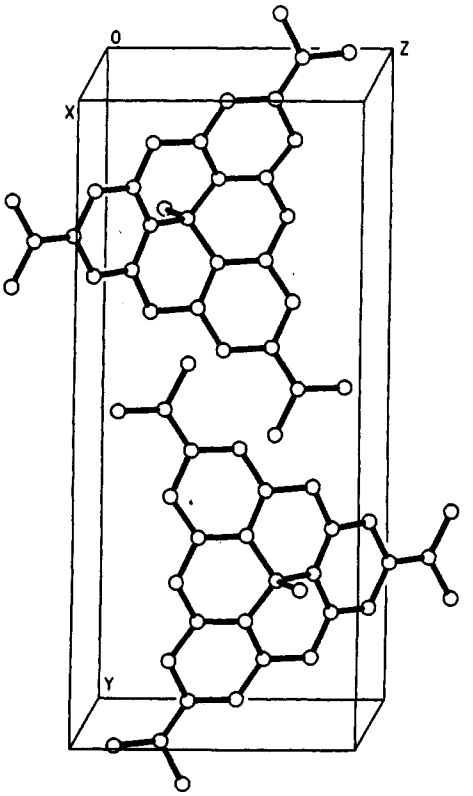

Figure 7. Unit cell diagram of **20**.

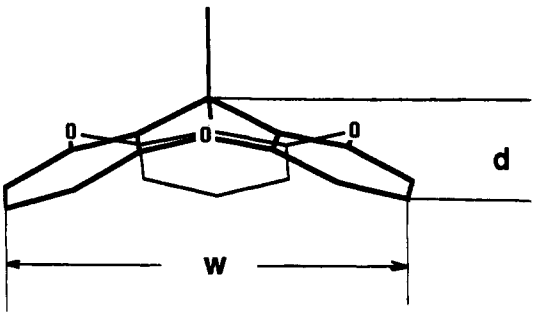

Figure 8. Parameter legend for Table II.

^{1}H NMR techniques to have a void inside the cage (Figure 5).[28]

Crystal Structure of 7. Crystals of **7** were grown from benzene. Room-temperature data were collected, and the structure was solved and refined in the space group $P2_1/n$ with four molecules per unit cell. Though the molecules sit in general positions and are slightly distorted from packing forces, they retain a geometry consistent with a molecular symmetry of C_{3v} in solution (Figure 6).

Crystal Structure of 20. Crystals of **20** were grown from benzene. Room temperature data were collected, and the structure was solved and refined in the space group $P2_1/c$ with four molecules per unit cell (Figure 7). The three nitrogens are almost planar, with an average sum of bond angles at the nitrogen of 358°. In the cyclophane **23** the nitrogens tend to be more pyramidal, with an average sum of bond angles of 347°. The difference is likely due to structural requirements imposed by the connected benzene ring in the cyclophane **23**.

The keystone unit can be viewed as a shallow bowl. The rim of the bowl is defined as the circle created by the three aromatic carbons para to the central position. The depth

(28) Lofthagen, M.; Chadha, R. K.; Siegel, J. S. *J. Am. Chem. Soc.*, in press.

Scheme V

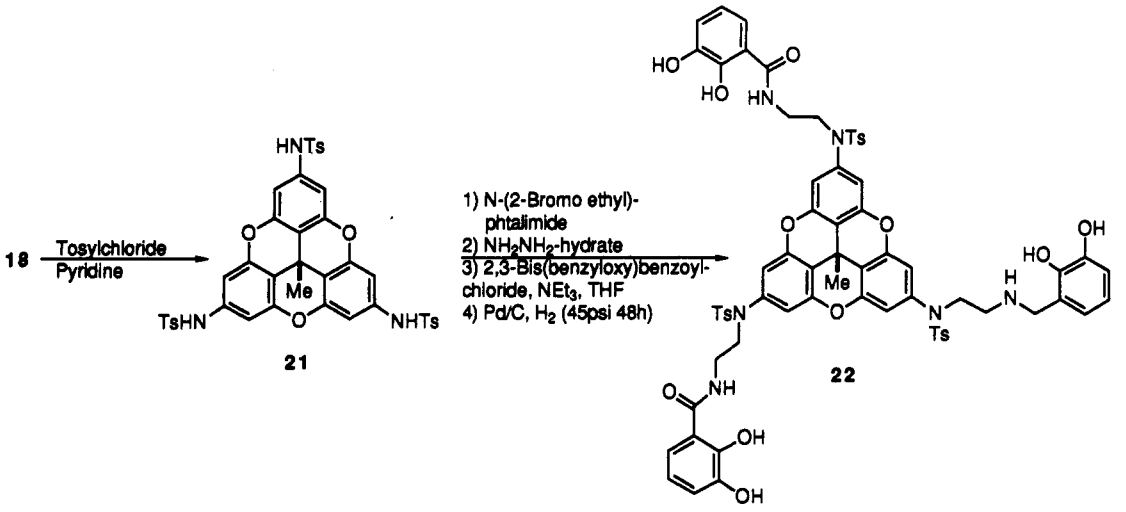

Scheme VI

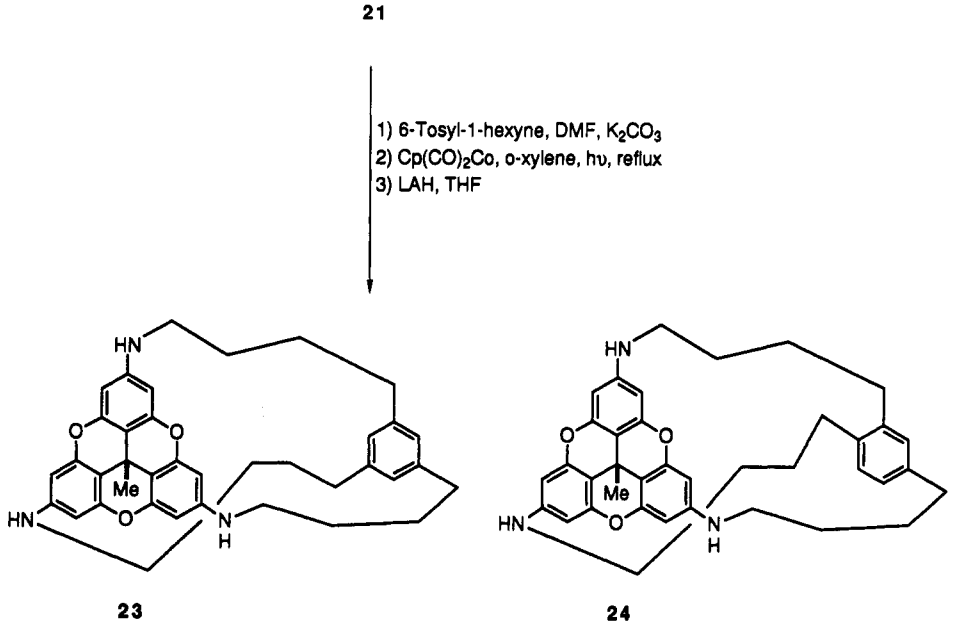

of the bowl is the distance from the rim plane to the quaternary carbon. An analysis of the crystal structures shows the depth of the keystone bowls in **7**, **20**, and **23**[27] are 1.32, 1.34, and 1.74 Å, respectively. Comparison with 1,1,1-triphenylethane (TPE),[29] which can be considered as a bowl filled in by its ortho and meta substituents, reveals a bowl depth of 1.44 Å, greater than both **7** and **20** (Figure 8, Table II).

An indication of strain in **7** and **20** is the phenyl ring distortion. Each of the aromatic rings in **7** and **20** shows the characteristic four up and two down distortions of a boat geometry.[30] In **7** the average out-of-plane distance for the "outer" aromatic carbon (i.e., 2, 6, 10) is 0.018 Å and for the "inner" aromatic carbon (i.e., 4b, 8b, 12b) it is 0.052 Å. The values for **20** are 0.035 and 0.066 Å, respectively. There is no such regular distortion in **23** or the TPE structure. The direction of these boat distortions in **7** and **20** leads to an overall flattening of the bowl, thus partly explaining the difference between the depth of the bowls in the keystones **7** and **20** and TPE.

Table II. Experimental and Calculated (EFF and AM1) Structures of 7, 20, 23, and TPE

		d	w	C_q–C_{Me} (Å)	oop[a]	oop[b]	C_{Ar}–C_q (Å)	C_{Ar}–C_q–C_{Me} (deg)
7	exp	1.32	7.01	1.55	0.052	0.018	1.498	110.5
	EFF	1.51	6.97	1.54			1.50	110.7
	AM1	1.35	7.02	1.53			1.49	110.2
20	exp	1.34	7.06	1.54	0.066	0.035	1.492	111.1
	EFF	1.59	6.96	1.59			1.50	111.7
	AM1	1.38	7.08	1.53			1.49	110.3
23	exp	1.74	6.80	1.54			1.496	111.4
	EFF	1.75	6.81	1.53			1.50	112.8
	AM1	1.74	6.80	1.53			1.50	110.8
TPE	exp	1.44	7.08	1.55			1.537	109.0
	EFF	1.41	7.15	1.55			1.53	108.9

[a] Average out of plane distance for carbons 4b, 8b, 12b. [b] Average out of plane distance for carbons 2, 6, 10.

The quaternary carbon in **7**, **20**, and **23** has shorter bond lengths to all substituents than TPE.[31] The average C(q)–C(ar) distance is 1.50 Å in **7**, **20**, and **23** and 1.54 Å in TPE. Surprisingly, the C(q)–C(me) distances at 1.55 Å are essentially equal for the four compounds; one would

(29) Destro, R.; Pilati, T.; Simonetta, M. *Acta Crystallogr.* **1980**, *B36*, 2495.

(30) Chance, J. M.; Kahr, B.; Buda, A. B.; Siegel, J. S. *J. Am. Chem. Soc.* **1989**, *111*, 5940.

(31) For an up to date table of standard bond lengths, see: Allen, F. H.; Kennard, O.; Watson, D. G.; Brammer, L.; Orpen, A. G.; Taylor, T. *J. Chem. Soc., Perkin Trans. 2* **1987**, S1–S19.

expect the compression of the C(q)–C(ar) bonds in **7**, **20**, and **23** to lead to an elongation of the C(q)–C(me) bond.[32] A short C(q)–C(ar) bond length is also responsible for the more shallow bowl in the keystones **7** and **20**.

7, **20**, and **23** are also more pyramidal than TPE at C(q) with respect to the 3-fold axis. With the 3-fold axis as reference, the apical angles average 110.5° for **7**, 111.1° for **20**, 111.4° for **23**, and 109.0° for TPE. This is in spite of the fact that Martin's salt appears to be a more stable cation and radical than the triphenylmethyl system. The geometric restrictions imposed by the closed-polycyclic connectivity result in the observed geometry. Also, the steric bulk in TPE favors a smaller angle. In the cyclophane **23** the combined effects of a large apical angle and the absence of boat distortions in the aromatic rings result in a greater bowl depth, 1.74 Å, than TPE.

The packing structure reveals that the keystones pack concave face to concave face with a slight lateral displacement.

Comparison with Empirical Force Field and AM1 Calculated Structures. Calculations on **7**, **20**, **23**, and TPE are consistent with the observed X-ray structures. The bond lengths and bond angles are in good agreement with those found in the X-ray structure (Table I). The calculations successfully predict the increased apical angles seen in the crystal structures of the 2,6,10-substituted keystones **20** and **23** as compared with the parent keystone **7**. The calculated geometrical parameters fit well enough with the experimental findings to provide useful predictions of structure for future systems of this type.[33,34]

Charge-Transfer Complexation. Addition of tetracyanoethylene (TCNE) to **7** in dichloromethane results in the formation of a deep purple solution. The color comes from a charge-transfer complex between **7** (donor) and TCNE (acceptor). Qualitative comparison of the binding of TCNE to anisole, 1,3-dimethoxybenzene, 1,1,1-tris(4-methoxyphenyl)ethane (TMPE), and **7** shows that all have low binding affinities ($K < 50\ M^{-1}$) but that **7** and TMPE bind qualitatively stronger than the others.

A correlation of the charge transfer λ_{max} (TCNE as acceptor) and the ionization potential of methoxyaromatics exists.[35] Based on this correlation the ionization potential for **7** should be 8.3 eV (λ_{max} = 545 nm; CH_2Cl_2), a value close to the ionization potential of 1,3-dimethoxybenzene. Thus, one can view **7** as an electron-rich aromatic system with some polar character.

Experimental Section

General Data. Proton NMR spectra were recorded on a ^1H NMR spectrometer equipped with a Nicolet 1180E computer interfaced with an Oxford magnet operating at 360 MHz or on a GE/Nicolet QE300 spectrometer. Carbon NMR were recorded on a Varian 500, QE300 spectrometer or on a Nicolet NT200 operating at 125, 75, and 50 MHz, respectively. Infrared spectra were recorded on a Perkin-Elmer 1420 IR spectrometer. UV spectra were recorded on a Perkin-Elmer Lamda 6 UV spectrometer. Unless otherwise stated, commercial chemicals were used as supplied: 1,3-dimethoxybenzene; *n*-butyllithium 2.5 M in hexanes; ethylchloroformate; pyridine hydrochloride; tetrafluoroboric acid–diethyl ether complex; methyllithium; lithium bromide adduct; 1.5 M in diethyl ether; chlorotrimethylsilane; sodium amide (Aldrich Chemical Co); tetrahydrofuran; benzene; bromine; sodium thiosulfate; ammonium chloride; potassium carbonate; hydrazine hydrate; silica (100–200 mesh, 230–425 mesh) (Fisher scientific); *N*-(2-bromoethyl)phthalimide (Fluka AG); preparative TLC plates (1000 microns) (Analtech); anhydrous ammonia (Linde specialty gases). Sesquixanthydryl terafluoroborate **5** was prepared by the procedure reported by Martin.[12] The THF was distilled from sodium/benzophenone. Alkyllithium reactions were performed under standard dry conditions under argon atmosphere.

12c-Methyl-4,8,12-trioxatricornan (7). Methyllithium–lithium bromide adduct, 1.5 M in diethyl ether (20.1 mmol), was added over 10 min to a suspension of **5** (5.0 g, 13.4 mmol) in 100 mL of dry THF. After being stirred for 1 h the solution was quenched with 50 mL of dilute ammonium chloride. The organic phase was then washed with water and dried over sodium sulfate. Removal of the solvent under vacuum gives a solid. The yellow-brown solid was redissolved in hot benzene (10 mL/g of solid), and the solution was filtered hot. Evaporation of the solvent yields **7** (3.0 g, 73%). Recrystallization from benzene yields white crystals (mp 230–231 °C): ^1H NMR ($CDCl_3$) δ 7.22 (3 H, t, J = 8.3 Hz), 6.92 (6 H, d, J = 8.3 Hz), 1.53 (3 H, s); $^{13}C\{^1H\}$ NMR (DMSO-d_6) δ 151.54, 128.81, 113.98, 111.44, 31.59, 23.43; IR (KBr) 1608, 1458, 1259, 1008 cm^{-1}; UV (EtOH) λ_{max} 220 nm (ϵ = 32 000 $M^{-1}\ cm^{-1}$); MS (CI, high resolution) found 301.0855 (calcd for $C_{20}H_{13}O_3$ (MH^+) 301.0865). Anal. Calcd for $C_{20}H_{12}O_3$: C, 79.99; H, 4.03. Found: C, 79.82; H, 4.08.

12c-Ethenyl-4,8,12-trioxatricornan (8). In a 250-mL round-bottom flask was placed **5** (4.0 g, 10.8 mmol) and 90 mL of dry THF along with a Teflon stirbar. The orange suspension was stirred, under a static blanket of argon, while vinylmagnesium bromide 1.0 M in THF 40 mL (40 mmol) was added dropwise over 30 min. The mixture darkened, a gas evolved, and a yellow flocculent precipitate formed. After 7 h the reaction was carefully quenched with a saturated solution of ammonium chloride. Diethyl ether (ca. 30 mL) was added to facilitate layer separation. The water layer was extracted twice more with ether; the organic layers were combined and dried over magnesium sulfate. The solvent was removed under reduced pressure to give a yellow solid (2.29 g, 68%). Pure **8** can be obtained by flash chromatography on silica gel (230–425 mesh), with cyclohexane as eluent. Recrystallization from cyclohexane yielded long clear colorless crystals (mp 205–207 °C): ^1H NMR ($CDCl_3$) δ 7.25 (3 H, t, J = 8 Hz), 6.94 (6 H, d, J = 8 Hz), 5.96 (1 H, dd, J = 17, 10 Hz), 5.00 (1 H, d, J = 10 Hz), 4.53 (1 H, d, J = 17 Hz); $^{13}C\{^1H\}$ NMR ($CDCl_3$) δ 152.43, 140.50, 128.54, 113.46, 111.90, 111.37; IR (KBr) 1613, 1482, 1456, 1261, 1017, 787, 783 cm^{-1}; FABMS (high resolution) 313.0860 (calcd for $C_{21}H_{13}O_3$ (MH^+) 313.0865).

12c-(3-Propenyl)-4,8,12-trioxatricornan (9). A 250-mL round-bottom flask was charged with **5** (2.29 g, 6.16 mmol) and 15 mL of dry THF along with a Teflon stirbar. The orange suspension was stirred, under a static blanket of argon, while allylmagnesium bromide 1.0 M in diethyl ether 18.6 mL (18.6 mmol) was added dropwise over 30 min. The reaction was allowed to warm to room temperature and stirred overnight. The reaction was quenched with dilute aqueous ammonium chloride. The orange mixture separated into two layers. The layers were separated, and the aqueous layer was extracted twice with diethyl ether. The organic layers were combined, and the solvent was removed under reduced pressure to give a yellow solid. This was purified on a short column of silica with dichloromethane as eluent. The isolated yield of the white powder **9** was 1.5 g (75%) (mp 174–179 °C): ^1H NMR ($CDCl_3$) δ 7.19 (3 H, t, J = 8.3 Hz), 6.90 (6 H, d, J = 8.3 Hz), 5.62 (1 H, m), 4.95 (1 H, d J = 9.7 Hz), 4.75 (1 H, d, J = 16.9 Hz), 2.51 (2 H, d, J = 7.2 Hz); $^{13}C\{^1H\}$ NMR ($CDCl_3$) δ 152.05, 130.94, 127.70, 119.26, 112.70, 110.67, 48.70, 28.83; IR (KBr) 1609, 1487, 1455, 1262, 1065, 1011 cm^{-1}; FABMS (high resolution) 327.1001 (calcd for $C_{22}H_{15}O_3$ (MH^+) 327.1021).

12c-(2-Oxopropyl)-4,8,12-trioxatricornan (10). **5** (500 mg, 1.34 mmol) and triethylamine (136 mg, 1.34 mmol) was refluxed for 18 h in 25 mL of acetone, yielding a slightly cloudy yellow solution. The acetone was removed under reduced pressure, and the solid residue was dissolved in 100 mL of a 1:1 mixture of THF and diethyl ether. The organic solution was extracted with water, dried with sodium sulfate, and evaporated to give **10** (390 mg, 85%) as a pale yellow solid. Pure **10** can be obtained by re-

(32) (a) Burgi, H.-B.; Dunitz, J. D. *Acc. Chem. Res.* **1983**, *16*, 153. (b) Burgi, H.-B. *Inorg. Chem.* **1973**, *12*, 2321. (c) Pauling, L. *Nature of the Chemical Bond*, *3rd ed.*; Cornell University Press: Ithaca, 1960.

(33) Empirical force field calculations were done using the program PCMODEL. AM1 calculations were done using MOPAC.

(34) PCMODEL is available through Kevin Gilbert at Serena Software.

(35) (a) Zweig, A. *J. Phys. Chem.* **1963**, *67*, 506. (b) Zweig, A.; Hodgson, W. G.; Jura, W. H. *J. Am. Chem. Soc.* **1964**, *86*, 4124. (c) Kampar, V. E. *Russ. Chem. Rev.* **1982**, *51*, 109.

crystallization from benzene (mp 204–205 °C): ^{1}H NMR ($CDCl_3$) δ 7.26 (3 H, t, J = 8.2 Hz), 6.95 (6 H, d, J = 8.2 Hz), 2.84 (2 H, s), 1.77 (3 H, s); $^{13}C\{^1H\}$ NMR ($CDCl_3$) δ 204.94, 152.56, 128.69, 111.94, 111.45, 55.55, 31.60, 27.52; IR (KBr) 1705, 1612, 1258 cm^{-1}; MS (DCI, high resolution) found 341.0796 (calcd for $C_{22}H_{13}O_4$ (M − H) 341.0814).

Hydroboration of 8. A two-neck 50-mL round-bottom flask, fitted with a dropping funnel and stirbar, was charged with 312 mg of **8** and dry THF (6 mL). The reaction was run under a static blanket of argon. The flask was placed in an ice–water bath, and 1.0 M borane in THF (3 mL) was added dropwise by syringe over a 45-min interval until hydrogen evolution was no longer seen. After this time, 3 M aqueous sodium hydroxide (3 mL) was added all at once. The organoborinic acid intermediate was oxidized by slow, careful dropwise addition of 30% H_2O_2 at a rate to maintain the temperature below 40 °C. The reaction mixture was allowed to stir for an additional 1 h to ensure complete reaction. Sodium chloride solid was added to facilitate separation of the THF layer. The THF layer was dried over magnesium sulfate and evaporated under reduced pressure to yield a white powder (90% crude yield). The primary and secondary alcohols were separated by flash chromatography on silica gel (230–425 mesh) with dichloromethane as eluent. Relative amounts of primary to secondary alcohols by ^{1}H NMR integration were 3.6:1. **Primary alcohol** (mp 182–185 °C): ^{1}H NMR ($CDCl_3$) δ 7.29 (3 H, t, J = 8 Hz), 6.93 (6 H, d, J = 8 Hz), 3.59 (2 H, td, J = 6, 7 Hz, respectively), 2.12 (2 H, t, J = 7 Hz), 1.01 (1 H, t, J = 6 Hz); $^{13}C\{^1H\}$ NMR ($CDCl_3$) δ 152.51, 128.34, 113.37, 113.06, 58.58, 47.01, 26.76; IR (KBr) 3307, 2945, 1613, 1481, 1456, 1263, 1054, 1034, 1013, 805, 790, 774, 762, 744 cm^{-1}; FABMS (high resolution) 331.0960 (calcd for $C_{21}H_{15}O_4$ (MH^+) 331.0970).

Secondary alcohol: mp 233–234 °C dec: ^{1}H NMR ($CDCl_3$) δ 7.27 (3 H, t, J = 8 Hz), 6.94 (6 H, d, J = 8 Hz), 3.95 (1 H, dt, J = 6, 7 Hz, respectively), 1.68 (1 H, d, J = 6 Hz), 1.06 (3 H, d, J = 7 Hz); $^{13}C\{^1H\}$ NMR ($CDCl_3$) δ 153.02, 152.84, 128.73, 111.34, 111.19, 110.17, 77.50, 34.82, 16.45; IR (KBr) 3500, 1613, 1483, 1459, 1265, 1102, 1068, 1015, 785, 733 cm^{-1}; FABMS (high resolution) 331.0973 (calcd for $C_{21}H_{15}O_4$ (MH^+) 331.0970).

1,7,9-Triamino-12c-methyl-4,8,12-trioxatricornan (11) and 1,5,9-Triamino-12c-methyl-4,8,12-trioxatricornan (12). **7** (1.0 g, 3.3 mmol) in 20 mL of concentrated nitric acid was heated at 90 °C for 2 h. The solution, containing a yellow precipitate, was then poured into 200 mL of ice–water. The yellow precipitate was collected by filtration and washed with several portions of water, yielding ca. 1.1 g of crude trinitro-substituted keystone. The material is only sparingly soluble in most organic solvents. To the crude mixture was added 320 mL of ethanol, 5 mL of hydrazine hydrate, and 0.245 g of 10% Pd/C. The solution was refluxed for 5 h under a static blanket of argon after which the insoluble materials has dissolved. The solvent was then removed under reduced pressure, and the resulting solid was extracted with 200 mL of methylene chloride. The solid was removed by filtration, and the orange-red filtrate was evaporated to yield 0.72 g of an amorphous solid containing **11** and **12** in a 3:1 ratio (determined by HPLC). The isomers were separated on neutral alumina (Mesh 150, Aldrich) eluting with (1) 1.5% methanol in methylenechloride, (2) 5% methanol in methylenechloride, yielding in the more polar solvent system (0.300 g) of **11**, and in the less polar solvent system 0.110 g of **12** (36% overall yield based on **7**).

1,7,9-Triamino-12c-methyl-4,8,12-trioxatricornan (11): mp > 190 °C dec; ^{1}H NMR ($CDCl_3$) δ 6.80–6.62 (6 H, m), 3.70 (6 H, s), 1.54 (3 H, s); $^{13}C\{^1H\}$ NMR (DMSO-d_6) δ 142.84, 142.27, 141.77, 138.62, 137.76, 137.69, 132.72, 132.26, 131.89, 114.73, 114.58, 114.47, 113.11, 112.80, 112.70, 110.53, 110.22, 109.65, 31.49, 24.78; IR (KBr) 3380, 3310, 1500, 1450, 1275, 1240, 1230, 1010 cm^{-1}; FABMS (high resolution) found 345.1120 (calcd for $C_{20}H_{15}N_3O_3$ (M^+) 345.1113).

1,5,9-Triamino-12c-methyl-4,8,12-trioxatricornan (12): mp > 200 °C dec; ^{1}H NMR ($CDCl_3$) δ 6.75 (6 H, d, J = 8.5 Hz), 6.63 (6 H, d, J = 8.5 Hz), 3.80 (6 H, s), 1.52 (3 H, s); $^{13}C\{^1H\}$ NMR (DMSO-d_6) δ 142.30, 138.51, 132.36, 114.58, 113.03, 110.05, 31.42, 24.80; IR (KBr) 3430, 3340, 1630, 1610, 1500, 1450, 1275, 1235, 1010 cm^{-1}; FABMS (high resolution) found 345.1120 (calcd for $C_{20}H_{15}N_3O_3$ (M^+) 345.1113).

1,7,9-Tris(trimethylsilyl)-12c-methyl-4,8,12-trioxatricornan (15) and 1,5,9-Tris(trimethylsilyl)-12c-methyl-4,8,12-trioxatricornan (16). **7** (3.0 g, 10 mmol) was dissolved in 180 mL of dry THF. The solution was cooled in an ice bath and n-butyllithium, 2.5 M in hexanes (90 mmol), was rapidly added by syringe. After being stirred overnight the solution was cooled in an ice bath and neat freshly distilled trimethylsilyl chloride (110 mmol) was added by syringe over 10 min. The solution was stirred for 30 min and thereafter quenched by addition of 1 M aqueous ammonium chloride. The organic phase was separated and dried over sodium sulfate. Evaporation of the solvent yields 4.5 g of a mixture of **15** and **16** in a 6:1 ratio (determined by HPLC). The mixture was then separated for identification. Analytical samples of each of the components of the mixture were obtained by preparative TLC (1-mm silica, petroleum ether 40–60 eluent).

1,7,9-Tris(trimethylsilyl)-12c-methyl-4,8,12-trioxatricornan (15): ^{1}H NMR ($CDCl_3$) δ 7.37 (1 H, d, J = 7.9 Hz), 7.35 (1 H, d, J = 8.3 Hz), 7.29 (1 H, d, J = 7.9 Hz), 6.93–6.91 (3 H, m), 1.47 (3 H, s), 0.419 (9 H, s), 0.417 (9 H, s), 0.366 (9 H, s); $^{13}C\{^1H\}$ NMR (acetone-d_6) δ 157.9, 154.2, 153.9, 135.7, 134.7, 121.9, 114.5, 114.2, 111.9, 111.7, 32.5, 0.833, −0.616; IR (KBr) 2952, 2899, 1605, 1282, 1248, 1208, 841 cm^{-1}; MS (CI, high resolution) found 516.1965 (calcd for $C_{29}H_{36}O_3Si_3$ (M^+) 516.1972). Anal. Calcd for $C_{29}H_{36}O_3Si_3$: C, 67.39; H, 7.02. Found: C, 67.51; H, 6.91.

1,5,9-Tris(trimethylsilyl)-12c-methyl-4,8,12-trioxatricornan (16): recrystallized from absolute ethanol (mp 163–165 °C); ^{1}H NMR ($CDCl_3$) δ 7.29 (3 H, d, J = 8.0 Hz), 6.90 (3 H, d, J = 8.0 Hz), 1.54 (3 H, s), 0.363 (27 H, s); $^{13}C\{^1H\}$ NMR ($CDCl_3$) δ 156.99, 153.78, 133.36, 121.46, 114.05, 110.88, 31.01, −0.682; IR (KBr) 2950, 1606, 1249, 841 cm^{-1}; MS (CI, high resolution) found 517.2013 (calcd for $C_{29}H_{37}O_3Si_3$ (MH^+) 517.2051).

1,11-Bis(trimethylsilyl)-12c-methyl-4,8,12-trioxatricornan (17). A small amount of the 1,11-bis substituted product was also isolated (<10%). Recrystallized from absolute ethanol (mp 176–178 °C): ^{1}H NMR ($CDCl_3$) δ 7.36 (2 H, d, J = 8.2 Hz), 7.21 (1 H, t, J = 8.2 Hz), 6.93 (2 H, d, J = 8.2 Hz), 6.90 (2 H, d, J = 8.2 Hz), 1.47 (3 H, s), 0.424 (18 H, s); MS (CI, high resolution) found 445.1624 (calcd for $C_{26}H_{29}O_3Si_2$ (MH+) 445.1655). Determination of regiochemistry by 1-D NOE subtraction ^{1}H NMR spectra. Saturation of resonance at 0.424 results in a ca. +10% NOE on resonance at 7.34. For **16**, saturation at 0.363 results in a +5% NOE at 6.90, as well as at 7.29 (+10%). Anal. Calcd for $C_{26}H_{28}O_3Si_2$: C, 70.23; H, 6.35. Found: C, 69.80; H, 6.33.

1,7,9-Tribromo-12c-methyl-4,8,12-trioxatricornan (13) and 1,5,9-Tribromo-12c-methyl-4,8,12-trioxatricornan (14). Procedure A. The crude mixture of **15** and **16** (4.54 g, from 3.0 g of **7**) was dissolved in 300 mL of dry THF and cooled in an ice bath. Bromine (29 mmol) was added quickly to the cooled solution. The solution was then allowed to warm to room temperature and stirred for a total of 3 h. Excess bromine was quenched by addition of a solution of sodium thiosulfate. The organic layer was dried over sodium sulfate, and the solvent was evaporated under reduced pressure to give an oily solid. Acetone (20 mL) was added to give a dark solution and tan precipitate. The resulting tan powder was filtered and washed with 3 × 2 mL portions of acetone yielding 2.74 g of **13** (51% based on **7**). An analytically pure sample can be obtained by recrystallization from acetone, yielding white needles (mp 224–227 °C): ^{1}H NMR ($CDCl_3$) δ 7.48 (3 H, m), 7.00 (1 H, d, J = 8.7 Hz), 6.89 (1 H, d, J = 8.7 Hz), 6.87 (1 H, d, J = 8.6 Hz), 1.53 (3 H, s); $^{13}C\{^1H\}$ NMR ($CDCl_3$) δ 151.03, 150.88, 150.78, 148.53, 131.77, 115.49, 115.20, 114.87, 113.50, 113.12, 112.83, 104.59, 104.20, 103.83, 31.67, 25.91; IR (KBr): 1605, 1476, 1448, 1285, 1258, 1010 cm^{-1}; FABMS (high resolution) found 533.8108 (calcd for $C_{20}H_9O_3Br_3$ (M^+) 533.8102). Anal. Calcd for $C_{20}H_9Br_3O_3$: C, 44.73; H, 1.69. Found: C, 44.80; H, 1.48.

The filtrate was flash-chromatographed (silica 100–200 mesh) eluting with hexanes to give 0.25 g, (mp 204–207 °C) of **1,5,9-tribromo-12c-methyl-4,8,12-trioxatricornan (14):** ^{1}H NMR ($CDCl_3$) δ 7.49 (3 H, d, J = 8.8 Hz), 6.99 (3 H, d, J = 8.8 Hz), 1.53 (3 H, s); $^{13}C\{^1H\}$ NMR ($CDCl_3$) δ 150.92, 148.39, 131.77, 115.16, 113.21, 104.24, 31.77, 25.92; IR (KBr): 1605, 1477, 1447, 1263, 1023 cm^{-1}; FABMS (high resolution) found 533.8085 (calcd for $C_{20}H_9O_3Br_3$ (M^+) 533.8102). Anal. Calcd for $C_{20}H_9Br_3O_3$: C, 44.73; H, 1.69. Found: C, 44.83; H, 1.68.

Procedure B: To **7** (3.00 g, 10 mmol) was added 150 mL of glacial acetic acid. The slurry was heated to 80 °C when most

of the solid dissolved. Bromine 8.0 g (50 mmol) in 40 mL of glacial acetic acid was then added dropwise over 30 min. The solution was heated for an additional 15 min. The solution was poured into 500 mL of ice–water. The resulting tan solid was isolated by filtration and washed with several portions of water. This crude product contain **13** and **14** in approximately a ratio of 3:1 (determined by ^{1}H NMR integration) also ca. 15% of tetrabromo-substituted **7** (identified by MS and quantified by ^{1}H NMR integration). This mixture was reacted on without further purification. However, isolation of pure **13** can be achieved by crystallization from 40 mL of acetone yielding 2.28 g (42%). **14** can be isolated by flash chromatography on silica (described above) from the C_3-enriched filtrate.

2,6,10-Triamino-12c-methyl-4,8,12-trioxatricornan (18). Procedure A. Into a round-bottomed flask containing 15 g of sodium amide was condensed 250 mL of ammonia. The crude reaction mixture of **13** and **14** from 3.00 g (10 mmol) of **7** was dissolved in 120 mL of dry THF and added dropwise over 30 min to the dry ice/acetone cooled ammonia solution. The solution was then transferred into a Parr stainless steel pressure reactor (600 mL capacity), cooled with dry ice/acetone. The reactor was closed, and the solution was stirred at room temperature for 24 h. The ammonia gas was released, and to the dark mixture was added 15 g of solid ammonium chloride. The solution was filtered and the bomb was washed out three times with 50 mL of diethyl ether. The dark red filtrate was evaporated in vacuo yielding a solid material. The crude product was chromatographed on Alumina (neutral, 150 mesh) eluting with methylenechloride/methanol (1000:36 mL) yielding 1.27 g of **18** (37% overall yield based on **7**, 2 steps) (mp > 300 °C dec): ^{1}H NMR ($CDCl_3$) δ 6.23 (6 H, s), 3.70 (6 H, s), 1.40 (3 H, s); $^{13}C\{^1H\}$ NMR (DMSO-d_6) δ 152.37, 149.02, 103.54, 96.51, 32.27, 21.56; IR (KBr) 3456, 3371, 1627, 1159 cm^{-1}; UV (ethanol) λ_{max} 224 nm (ϵ = 86 400 M^{-1} cm^{-1}); MS (CI, high resolution) found 346.1215 (calcd for $C_{20}H_{16}N_3O_3$ (MH^+) 346.1192). Anal. Calcd for $C_{20}H_{15}N_3O_3$: C, 69.56; H, 4.38; N, 12.17. Found: C, 68.92; H, 4.22; N, 12.14.

Earlier fractions gave **2,6-diamino-12c-methyl-4,8,12-trioxatricornan (19)**: mp > 245 °C dec ^{1}H NMR ($CDCl_3$) δ 7.16 (1 H, t, J = 8.2 Hz), 6.86 (2 H, d, J = 8.2 Hz), 6.28–6.22 (4 H, m), 3.72 (4 H, s), 1.44 (3 H, s); $^{13}C\{^1H\}$ NMR ($CDCl_3$) δ 153.00, 152,87, 152.38, 146.71, 127.46, 115.88, 111.09, 105.74, 98.33, 98.19, 31.78; IR (KBr) 3456, 3371, 1630, 1618, 1470, 1254, 1161 cm^{-1}; FABMS (high resolution) found 331.1079 (calcd for $C_{20}H_{15}N_2O_3$ (MH^+) 331.1083). Anal. Calcd for $C_{20}H_{14}N_2O_3$: C, 72.72; H, 4.27; N, 8.48. Found: C, 71.65; H, 4.38; N, 8.14.

2,6,10-Triamino-12c-methyl-4,8,12-trioxatricornan (18). Procedure B: A 200-mL sealable tube, cooled with dry ice/acetone, was charged with sodium amide (2.1 g) and 40 mL of liquid ammonia. The solution was cooled with dry ice/acetone. **13** (1.40 g, 2.61 mmol) dissolved in 20 mL of dry THF was added to the cooled solution. The tube was sealed and solution stirred at room temperature for 19 h. The tube was cooled again to dry ice/acetone temperature and reopened. To the dark solution was added 2 g of ammonium chloride solid, the ammonia THF mixture was evaporated by passing argon through the solution at room temperature to leave a gummy product. The gummy residue was extracted with several portions of diethyl ether. The pale orange ethereal solution was evaporated to give an orange solid. The crude product 0.9 g was chromatographed as described in procedure A, to give 0.51 g (57% yield based on **13**, 1 step) of **18**.

Earlier fractions gave 40 mg of **2,6-diamino-12c-methyl-4,8,12-trioxatricornan (19)**.

2,6,10-Tris(dimethylamino)-12c-methyl-4,8,12-trioxatricornan (20). Into a 200-mL round-bottomed flask, cooled with dry ice/acetone, was condensed 30 mL of dimethylamine. Into this was added 38 mL of a 2.5 M solution of n-BuLi in hexanes. The solution was transferred into a Parr stainless steel pressure reactor (600-mL capacity) and a slurry of crude "tribromides" **13** and **14** (2.15 g) in 16 mL of dry THF was added. The reactor was closed, and the solution was stirred at room temperature for 48 h. Excess dimethylamine was evaporated, and the solution was diluted with diethyl ether and extracted with a saturated ammonium chloride solution followed by water. The organic solution was dried with sodium sulphate and evaporated. The mixture was flash chromatographed (silica, 230–425 mesh) eluting with chloroform to yield 0.22 g (13% based on the tribromide) of **20**: mp 255 °C dec; ^{1}H NMR ($CDCl_3$) δ 6.29 (6 H, s), 2.95 (18 H, s), 1.46 (3 H, s); $^{13}C\{^1H\}$ NMR ($CDCl_3$) δ 152.73, 150,38, 104.41, 95.34, 40.36, 31.19, 21.86; IR (KBr) 2940, 1625, 1585, 1245, 800 cm^{-1}; FABMS (high resolution) found 430.2120 (calcd for $C_{26}H_{28}N_3O_3$ (M^+) 430.2131).

X-ray Crystallography. Crystals of 12c-methyltrioxatricornan **7** were grown from benzene by slow cooling of a warm saturated solution. A colorless parallelopiped of approximately 0.16 × 0.17 × 0.37 mm was chosen for the X-ray measurements. Crystal data: $C_{20}H_{12}O_3$, M = 300.3 g/mol; monoclinic (spacegroup $P2_1/n$); a = 8.546 (3) Å, b = 16.314 (7) Å, c = 10.249(4) Å, β = 101.38 (3)°; V = 1400.9 (10) Å^3; d_{calc} = 1.42 g·cm^{-3}; Z = 4. X-ray intensities were recorded at room temperature on a Nicolet R3m/v four circle diffractometer using Cu Kα radiation (λ = 1.541 84 Å). A total of 1753 independent reflections were collected with 4° < 2θ < 110°, of which 1605 with $|F0|>3\sigma$ ($F0$) were considered unique and observed. The structure was solved by direct methods with the SHELXTL PLUS software.[36] All non-hydrogen atoms were refined anisotropically using a full matrix least-squares procedure. Hydrogen atoms were included at ideal positions. The data to parameter ratio was 7.7:1 and after refinement the R and R_w factors were 7.97 and 9.29, respectively. The largest residual peak in the final Fourier difference map was 0.41 e/Å^3.

Crystals of 2,6,10-tris(dimethylamino)-12c-methyltrioxatricornan (**20**) were grown from benzene by slow cooling of a warm saturated solution. A colorless parallelopiped of approximately 0.25 × 0.37 × 0.55 mm was chosen for the X-ray measurements. Crystal data: $C_{26}H_{27}N_3O_3$, M = 429.5 g/mol; monoclinic (space group $P2_1/c$); a = 7.569 (2) Å, b = 18.392 (8) Å, c = 8.007 (3) Å, β = 98.87 (3)°; V = 1101.3 (7) Å^3; d_{calc} = 1.30 g·cm^{-3}; Z = 2. X-ray intensities were recorded at room temperature on a Nicolet R3m/v four circle diffractometer using Cu Kα radiation (λ = 1.541 84 Å). A total of 2007 independent reflections were collected with 4.5° < 2θ < 50.0°, of which 1484 with $|F0|>3\sigma$ ($F0$) were considered unique and observed. The structure was solved by direct methods with the SHELXTL PLUS software. All non-hydrogen atoms were refined anisotropically using a full matrix least-squares procedure. Hydrogen atoms were included at ideal positions. The data to parameter ratio was 9.6:1 and after refinement the R and R_w factors were 5.35 and 7.07, respectively. The largest residual peak in the final Fourier difference map was 0.30 e/Å^3.

Acknowledgment. We would like to thank the NSF PYI award program (CHE-8857812) and American Cancer Society Jr Faculty Fellowship (C-58024) for support. We greatly appreciate additional support of our program from the Exxon Educational Fund, Hofmann La Roche, Rohm+Haas, Monsanto, Eli Lilly, Zambon Italia, and Sterling Drug. We would also like to thank Raj Chadha for technical assistance in solving the X-ray structures of **7** and **20**. Funds for the 500-MHz NMR were provided by NIH (RR04733) and NSF (CHE8814866).

Supplementary Material Available: X-ray coordinates and thermal parameters; selected NMR spectra (44 pages). Ordering information is given on any current masthead page.

(36) SHELXTL plus is an advanced form of the SHELX solutions package and is available through Sieman's Instrument Co.